ELSEVIER

Journal of Power Sources 94 (2001) 102–107

JOURNAL OF POWER SOURCES

www.elsevier.com/locate/jpowsour

$Zn_4Sb_3(–C_7)$ powders as a potential anode material for lithium-ion batteries

G.S. Cao*, X.B. Zhao, T. Li, C.P. Lu

Department of Materials Science and Engineering, Zhejiang University, Hangzhou 310027, PR China

Received 7 February 2000; received in revised form 4 October 2000; accepted 6 November 2000

Abstract

The electrochemical properties of β-Zn_4Sb_3 and Zn_4Sb_3–C_7 as new lithium-ion anode materials were investigated. The reversible capacities of the pure Zn_4Sb_3 alloy electrode and 100 h milled Zn_4Sb_3 in the first cycle reached 503 and 566 mA h/g, respectively, but the cycle stability of Zn_4Sb_3 whether milled or not were obviously bad. It was demonstrated that cycle stability of Zn_4Sb_3 could be largely improved by milling after mixing with graphite. It was shown that Zn_4Sb_3–C_7 composite has a lithium-ion extraction capacity of 581 mA h/g at the first cycle and 402 mA h/g at 10th cycle.

Keywords: Zn_4Sb_3; Lithium-ion batteries; Anode materials

1. Introduction

Lithium-ion batteries are efficient secondary power supply for their high efficiency and high energy density, and show their potential large market applications from portable electronic devices to electric vehicles. For this reason, a lot of researches were reported in the recent years. As a rock-chair cell, the anode material greatly influences lithium-ion battery in both battery capacity and energy density. Up to the present, only graphite, modified graphite and hard carbon materials were used into lithium-ion battery anodes for commercial applications. Some shortcomings affected the further improvement of the properties and the applications of lithium-ion batteries. The theoretical capacity of graphite is only 372 mA h/g (LiC_6). Although some new super-high capacity graphite such as MCMB [1,2] and PBDC [3] were developed, their electrode potential after lithium-ion insertion are rather low, which affects the rapid charge/discharge behavior and safety behavior of lithium-ion batteries. It was reported that tin oxide-based materials have good theoretical capacities, about 782 mA h/g ($Li_{22}Sn_4$), but their irreversible capacities are rather large at the first cycle for the charge mechanism of tin oxides [4–6], $38Li^+ + 4SnO_2 + 38e^- \rightarrow Li_{22}Sn_4 + 8Li_2O$. Except for carbon, carbon-based materials and tin oxide-based materials, tin alloys [7,8] also show large capacity and small irreversible capacity in the first cycle, though, because tin alloys powders disintegrated during the lithium-ion inserting and extracting process, their cycle lives are obviously poor.

Some new possible lithium-ion batteries anode materials are recently reported for having reached a suitable reversible capacity and/or with an acceptable cycle life, for examples, silicon [9], Mg_2Ge [10], $Li_{2.6}Co_{0.4}N$ [11], MNb_2O_6 [12] and $Li_4Ti_5O_{12}$ [13]. It should be especially marked out that these anode materials have not included those conventional elements, i.e. carbon and tin. These anode materials have shown that the main advantages are more reversible capacity than carbon and less irreversible capacity than tin oxides, furthermore, the main shortcoming is the cycle life is poor. Therefore, to find new anode materials with both large reversible capacity and good cycle life becomes the important aim of lithium-ion battery researches.

Considering the fact that Sb has the chemical properties similar to Si and Sn, and Li^+-insertion capacity of 536 mA h/g (Li_3Sb) [14], some Sb-containing compounds could be the potential anode materials of lithium-ion batteries [15,16]. As a potential thermoelectric material, β-Zn_4Sb_3 has been studied for a few years [17,18]. It has a hexagonal rhombohedric crystal structure, with $a = 1.2231$ nm and $c = 1.2428$ nm. The relatively low density of β-Zn_4Sb_3 (6.077 g/cm^3) compared with pure Zn (7.14 g/cm^3) and Sb (6.684 g/cm^3) suggests that there should be more and/or larger space in the β-Zn_4Sb_3 crystal structures for lithium ions.

* Corresponding author.
E-mail address: gaosho@163.net (G.S. Cao).

0378-7753/01/$ – see front matter
PII: S0378-7753(00)00650-9

In the present study, we investigated the preparation and electrochemical properties of β-Zn_4Sb_3, 100 h ball-milled Zn_4Sb_3, the mixture of Zn_4Sb_3 and graphite, and Zn_4Sb_3–C_7. We found that Zn_4Sb_3–C_7 could be a potential lithium-ion battery anode material because of its reversible capacity and its acceptable cycle life.

2. Experiment methods

β-Zn_4Sb_3 was prepared with vacuum smelt method. Pure Zn powder (Wuhan, more than 99.0% pure) and pure Sb powder (Shanghai, more than 98.0% pure) with the atom ratio of 4:3 were sealed in a Ø 14 mm × 100 mm quartz glass tube with pressure of 10^{-2} Pa, and heated up to 750°C and maintained for 4 h. After then, the tube was quenched in water. The as-cast alloy was ground into 500 meshes fine powders. Some Zn_4Sb_3 powder was further milled in ligroin for 100 h without interrupt in a high-energy planetary ball mill (QM-1SP) at 120 rpm, and the weight ratio of stainless balls to alloy powders was 20:1. Using the same milling method, Zn_4Sb_3(–C_7) composite was prepared from pure Zn_4Sb_3 powder and graphite (Shanghai, more than 99.99% pure) with the mole ratio of 1:7.

Identification of phases and structures was carried out on these samples by X-ray diffraction (XRD) measurements using a Philips diffractometer PW1710 with Cu kα radial.

The testing electrodes were prepared by coating slurries of 95 wt.% respective alloy powders and 5 wt.% polytetrafluoroethylene (PTFE) on a foam nickel substrate with the size of Ø 10 mm × 1.5 mm. After coating, electrodes were pressed between steel plates at 18 Mpa for 1 min, and then dried at 110°C for 24 h. All electrochemical measurements are carried out using the cell model shown in Fig. 1. A lithium foil (Beijing, more than 99.9% pure) was used as counter electrode, and polypropylene paper (Celgard 2300) as the microporous separator. The organic electrolyte was prepared by dissolving 1 M vacuum dried $LiClO_4$ in 1:1 volume ratio mixture of ethylene carbonate (EC, Merck, more than 99.5% pure) and diethyl carbonate (DEC, Messerschmittstr, more than 99.5% pure). All cells were assembled in an Ar-filled glove box.

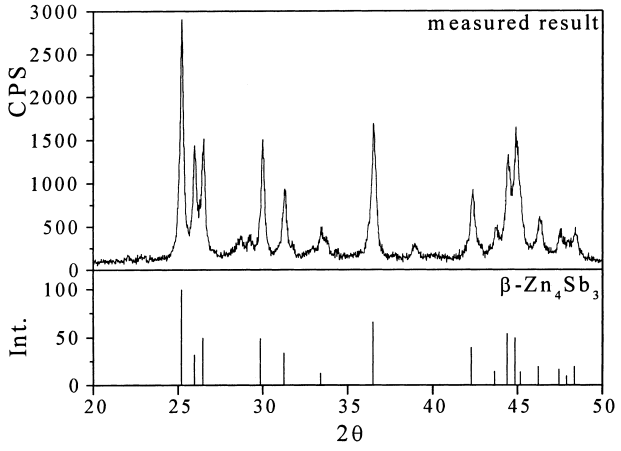

Fig. 2. The XRD result of Zn_4Sb_3 alloy.

A constant-current charge/discharge measuring instrument controlled by a computer was used to measure and analyze the electrochemical properties of the anode materials. The test temperature was stabilized at 30°C, and the current of charge or discharge was 40 mA/g typically. The relation of differential specific capacities with the electrode voltages, $dq/dV \sim V$, in units of A h/(g V), were calculated from the charge/discharge data. Because of the big polarization of researching electrodes, all charge/discharge voltages were set from 0.005 to 2.5 V.

3. Experimental results and analysis

A XRD diffraction pattern of Zn_4Sb_3 alloy powders is shown in Fig. 2. The spectrum lines of standard β-Zn_4Sb_3 [19] are also given with the maximum diffraction intensity being set as 100. It can be seen that a perfect β-Zn_4Sb_3 alloy has been obtained in the as-cast alloy. The peaks are very sharp. From the width of the diffraction peaks, the average grain size could be calculated according to the Scherrer equation: size $= k/\cos$. The estimated average crystallite size for the β-Zn_4Sb_3 alloy powders is larger than 100 nm. Fig. 3 shows the X-ray diffraction pattern of 100 h ball-milled Zn_4Sb_3 alloy powders. Comparing with the result of

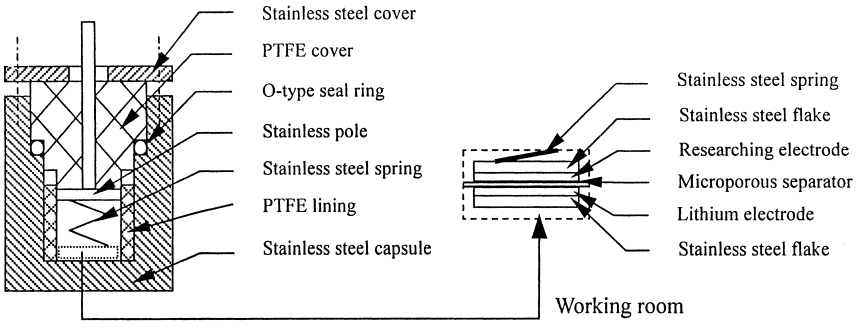

Fig. 1. Sketch of testing cell model.

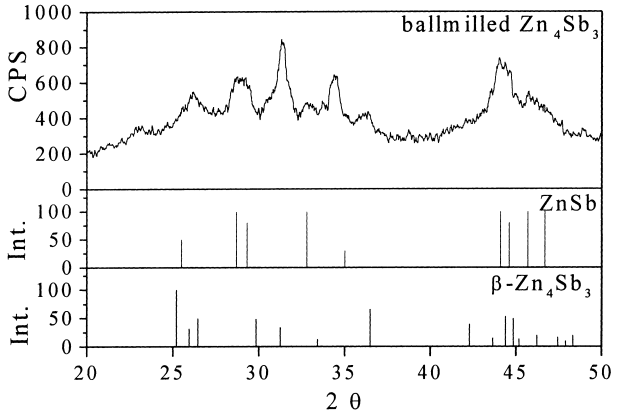

Fig. 3. The XRD result of ball-milled Zn_4Sb_3 alloy.

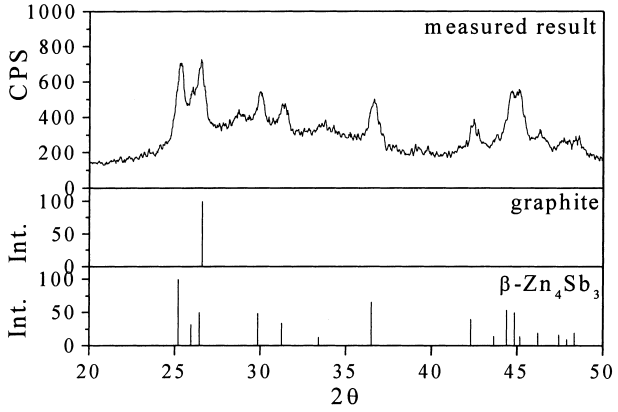

Fig. 4. The XRD result of ball-milled Zn_4Sb_3–C_7.

unmilled alloy, the XRD result of milled alloy shows largely reduced and broadened peaks. It can be found in Fig. 3 that some β-Zn_4Sb_3 alloy powders have been changed to ZnSb structure together with some other unknown structures after high-energy ball-milling. The XRD result of ball-milled Zn_4Sb_3–C_7 (Fig. 4) suggests it is a mixture of Zn_4Sb_3 alloy and graphite. Both Figs. 3 and 4 show that there are some amorphous phases in ball-milled powders.

Fig. 5 shows the electrochemical properties of unmilled Zn_4Sb_3 sample. The open-circuit potential of the Zn_4Sb_3 electrodes are in the range of 2.5–2.8 V versus Li/Li^+ in the unlithiated state. When lithium ions are inserted, the potential of the electrode quickly dropped to 1.5 V and lower. A first discharge capacity of 487 mA h/g was achieved, corresponding to the storage of 11.9 mol Li/mol of Zn_4Sb_3. One notices from Fig. 5a that the capacity of lithium ion extracting capacity (503 mA h/g) is higher than the inserting capacity in the first charge/discharge cycle. Chemical analysis after measurement shows that there is a certain amount of Zn and Sb elements in the electrolyte, which means that the dissolving of Zn and Sb ions from anode in the electrolyte might supply extra positive electrons during the lithium-ion extracting process. The following cycles show that both charge and discharge capacities decrease very fast. The differential capacity versus voltage curve of first cycle is given in Fig. 5b. A peak in Fig. 5b corresponds with a voltage plateau in Fig. 5a. It obviously shows two main Li^+ insertion plateaus at about 0.55 and 0.15 V. This suggests there are two main reactions of lithium-ion inserting into unmilled Zn_4Sb_3 anode. These Li^+ insertion plateaus are different from the reaction of lithium ion inserting into either Zn (about 0.2 V) or Sb (about 0.95 V) [14–16]. Only one main plateau is found at near 0.8 V in the extracting process. The small plateau found near 1.5 V might be caused by the extractions of alloy atoms.

Fig. 6 shows the electrochemical properties of 100 h ball-milled Zn_4Sb_3 sample. Compared with unmilled Zn_4Sb_3, the milled alloy shows significantly higher charge and discharge capacities. The first Li^+ inserting capacity is 680 mA h/g, and a first extracting capacity of 566 mA h/g is reached. Being similar to unmilled alloy, the milled alloy decreases its capacities very fast after the first cycle. The differential capacity versus voltage curve of first cycle is shown at Fig. 6b. Comparing with unmilled Zn_4Sb_3, the voltages of two main Li^+ inserting plateaus are increased, and furthermore, the plateau at about 0.85 V becomes remarkable, which suggests that milled alloy electrode has a lower resistance for lithium ions to insert into. At the first lithium

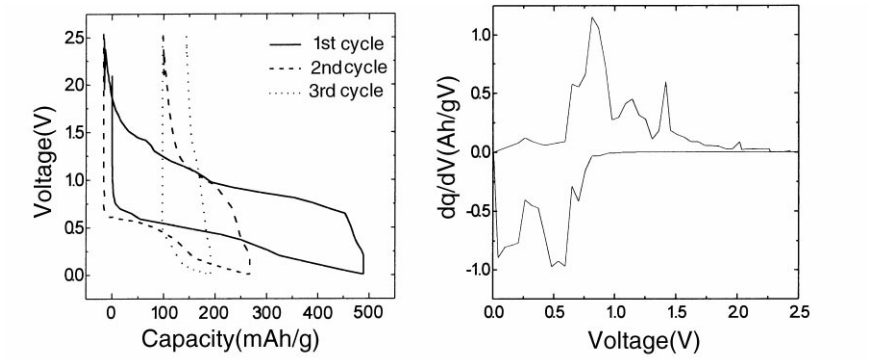

(a) Charge-discharge curves of the first three cycles (b) Differential capacities of the first cycle

Fig. 5. Charge–discharge properties of Zn_4Sb_3 alloy ($I_c = I_d = 40$ mA/g).

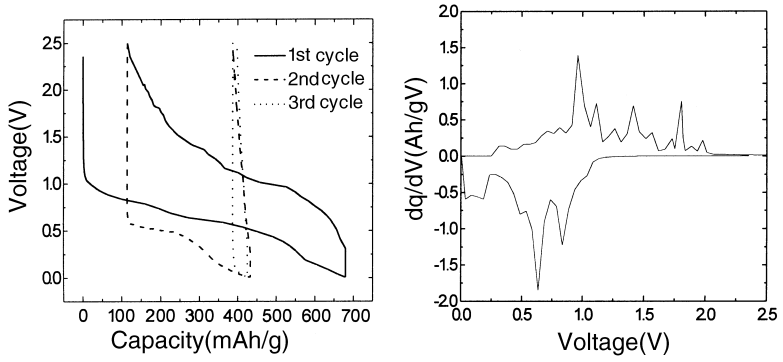

(a) Charge-discharge curves of the first three cycles (b) Differential capacities of the first cycle

Fig. 6. Charge–discharge properties of 100 h ball-milled Zn_4Sb_3 alloy ($I_c = I_d = 40$ mA/g).

extracting process, a main plateau is found at near 0.95 V, which is higher than the voltage of unmilled alloy.

Fig. 7 shows the electrochemical properties of Zn_4Sb_3–C_7 composite. One sees that the charge/discharge curves and the differential capacity curves of Zn_4Sb_3–C_7 are much smoother than those of both milled and unmilled Zn_4Sb_3 alloys. The capacity of Zn_4Sb_3–C_7 in the first cycle reaches 919 mA h/g for lithium ion inserting process and 581 mA h/g for extracting. Although the irreversible capacity is relatively large at the first cycle, it is much reduced after then. The long charge/discharge voltage plateaus and the reversible capacity of Zn_4Sb_3–C_7 suggest that it could be a potential anode material for lithium-ion batteries.

There are two Li^+ inserting plateaus at 0.06 V and near 0.85 V for Zn_4Sb_3–C_7 alloy electrode. The former fits the pure graphite charge potential very well. The later peak near 0.85 V, which exists also in unmilled and milled Zn_4Sb_3 samples (Figs. 5 and 6b), is the dominant plateau in the Zn_4Sb_3–C_7 sample. We consider it to be the "intrinsical" Li^+-inserting potential of Zn_4Sb_3, since there is no new phase in the Zn_4Sb_3–C_7 sample and even no significant change of the Zn_4Sb_3 crystal structure after ball-milled with graphite according to the XRD result.

According to the change of the inserting peak near 0.85 V from Figs. 5 to 7, the mechanism of lithium-ion inserting into Zn_4Sb_3 is based on the reaction of Zn_4Sb_3 with Li^+: $Zn_4Sb_3 + Li^+ \rightarrow LiZnSb + Zn$ [20]. In detail, we suggest lithium ions insert into Zn_4Sb_3 at about 0.85 V for all samples studied in the present work. For the sample of unmilled Zn_4Sb_3 with relative large grain size, however, due to the anode polarization caused by the crystal lattice stress after the inserting if lithium ions into the surface layers of grains and/or by the poor electrical contact between grains, only a small amount of lithium ions could insert into the anode material at the intrinsical potential, i.e. about 0.85 V versus Li/Li^+. Then, the most portions of lithium ions could be inserted into the anode only after the cracking of the Zn_4Sb_3 grains from the surface to inner layer by layer at the lower potential than 0.85 V. For the ball-milled Zn_4Sb_3, because of the fine grains, more lithium ions can be inserted into the surface layer of the anode material before the grain cracking. But also the milled Zn_4Sb_3 anode suffers from the polarization during the lithium ion inserting. The polarization of the anode can be eliminated by milling the alloy with graphite, which can largely improve the electrical contact between the grains in the electrode. It makes the lithium ions well distributed and uniformly among the Zn_4Sb_3 grains in the anode, so that the Li^+ inserting process of any grain in the anode becomes much easier and milder than the case without graphite.

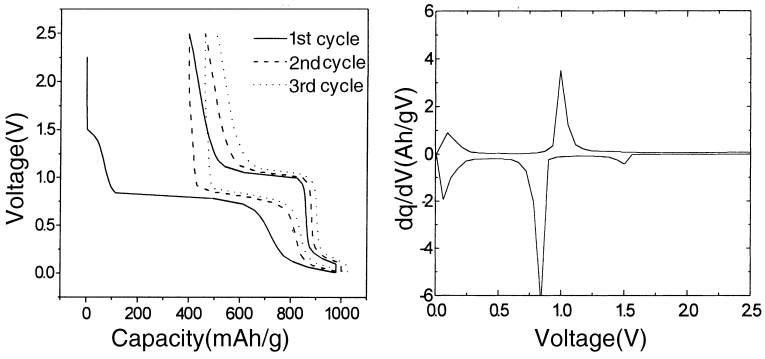

(a) Charge-discharge curves of the first three cycles (b) Differential capacities of the first cycle

Fig. 7. Charge–discharge properties of Zn_4Sb_3–C_7 composite ($I_c = I_d = 40$ mA/g).

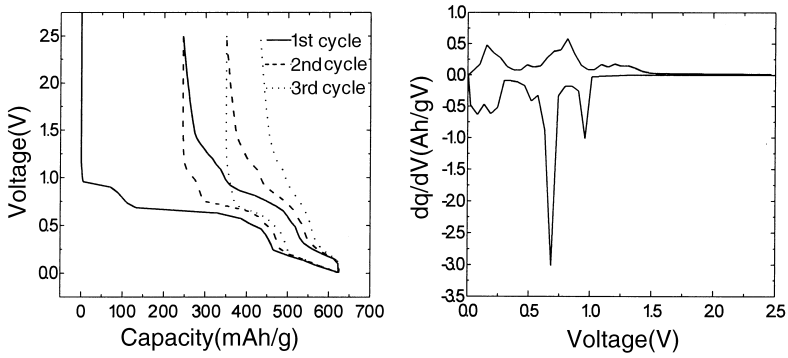

(a) Charge-discharge curves of the first three cycles (b) Differential capacities of the first cycle

Fig. 8. Charge–discharge properties of Zn_4Sb_3 mixed with graphite ($I_c = I_d = 40$ mA/g).

In comparison, Fig. 8 shows the electrochemical properties of Zn_4Sb_3 (mixed with graphite). The ratio is 1 mol Zn_4Sb_3: 7 mol carbon. Here, the graphite acts as carbon black that is widely used by other researchers. One sees that the charge/discharge curves and the differential capacity curves are smoother than that of Zn_4Sb_3 electrode without graphite and are similar in potential plateaus to Zn_4Sb_3–C_7. Nevertheless, though it mixed with graphite, Zn_4Sb_3 shows rapid capacity decrease.

Two peaks in the lithium-ion extracting curve (Fig. 7b) at about 0.1 and 1.0 V correspond with the processes of lithium ions extracting from graphite and Zn_4Sb_3, respectively. On comparing Fig. 7b with Figs. 5 and 6b, one sees that milled Zn_4Sb_3 and Zn_4Sb_3–C_7 have the similar extracting potential (almost 1.0 V), in contrast, unmilled Zn_4Sb_3 has a lower potential (at near 0.8 V). The change of Li^+ extracting peaks also proves the above mechanism we suggested, i.e. the unmilled Zn_4Sb_3 have serious crystal lattice stress after Li^+ completely being inserted into, it strongly leads the anode to unstable state. As a result, the lithium ions are easy to be extracted from, which means the extracting plateau potential of unmilled Zn_4Sb_3 is lower than milled anodes. The long charge/discharge voltage plateaus and the reversible capacity of Zn_4Sb_3–C_7 suggest that it could be a potential lithium-ion battery anode material.

Fig. 9 shows the cycle lives (lithium ion extracting capacities) of the unmilled and milled Zn_4Sb_3 alloy and Zn_4Sb_3–C_7 composite. The results show that although Zn_4Sb_3 alloys, whether it milled or not, have the capacities more than 500 mA h/g at the first cycle, lose their capacities very fast in the following cycles. Their reversible capacities are both lower than 10 mA h/g even after only five cycles. It is considered being caused by the dissolving of the anode atoms during the extraction of Li^+, which destroyed the crystalline structure of the anode materials. Fig. 9 also shows an acceptable cycling property of Zn_4Sb_3–C_7. It can be attributed to the addition of graphite, which, as discussed above, eliminates the polarization of the anode and minimizes the fracture of the anodes grains by wrapping and upholding the Zn_4Sb_3 in the anode.

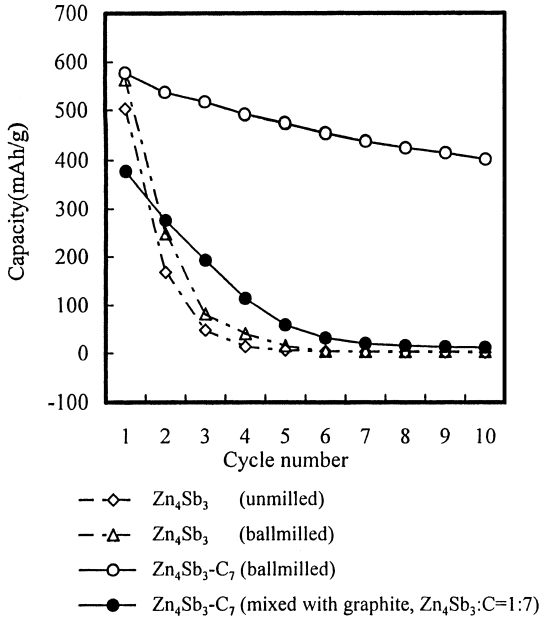

Fig. 9. Capacity of unmilled/milled Zn_4Sb_3, Zn_4Sb_3–C_7 and Zn_4Sb_3 (mixed with graphite) vs. cycle number (limited voltage is from 0.005 to 2.5 V, and currents is $I_c = I_d = 40$ mA/g).

4. Conclusions

The intermetallic compound Zn_4Sb_3 has a reversible lithium-ion charge/discharge capacity at the first cycle of 503 mA h/g. Nevertheless, the alloy shows a very poor electrochemical cycling life because of the destruction of the crystalline structure and the fracture of the grains of the alloy during the inserting/extracting of lithium ions.

Fining the grain sizes to about a few micrometers by milling the alloy for 100 h increases the capacity somewhat, but results no remarkable improvement in the cycling life of the alloy electrode.

Compositing the Zn_4Sb_3 powder with graphite by milling improves the cycling properties of the alloy significantly and increases its reversible capacity up to 581 mA h/g at the first cycle, although there are no new phases formed in the

composite. It is suggested that ball-milling with graphite can eliminate the anode polarization during the inserting of lithium ions and minimization the destruction of the crystalline structure of the alloy.

Acknowledgements

This work was partially supported by National Science Foundation of China (no. 59771032) and RFDP of the Education Ministry of China (no. 97033518).

References

[1] T. Zheng, Y. Liu, E.W. Fuller, S. Tseng, S.U. Von, J.R. Dahn, Lithium insertion in high capacity carbonaceous materials, J. Electrochem. Soc. 142 (8) (1995) 2581–2590.

[2] K. Sato, M. Noguchi, A. Demachi, N. Oki, M. Endo, A mechanism of lithium storage in disordered carbons, Science 264 (4) (1994) 556–558.

[3] N. TaKami, A. Satoh, T. Ohsaki, M. Kanda, Large hysteresis during lithium insertion into and extraction from high-capacity disordered carbons, J. Electrochem. Soc. 145 (2) (1998) 478–482.

[4] L. Weifeng, H. Xuejie, W. Zhaoxiang, L. Hong, C. Liquan, Studies of stannic oxide as an anode material for lithium-ion batteries, J. Electrochem. Soc. 145 (1) (1998) 59–62.

[5] Y. Idota, T. Kubota, A. Matsufuji, Y. Maekawa, T. Miyasaka, Tin-based aamorphous oxides: a high capacity lithium-ion-storage material, Science 276 (7) (1997) 1395–1397.

[6] T. Brousse, R. Retoux, U. Herterich, D.M. Schleich, Thin-film crystalline SnO_2–lithium electrodes, J. Electrochem. Soc. 145 (1) (1998) 1–4.

[7] O. Mao, R.A. Dunlap, J.R. Dahn, Mechanically alloyed Sn–Fe(–C) powders as anode materials for Li-ion batteries — the Sn_2Fe–C system, J. Electrochem. Soc. 146 (2) (1999) 405–413.

[8] K.D. Kepler, J.T. Vaughey, M.M. Thackeray, Copper–tin anodes for rechargeable lithium batteries: an example of the matrix effect in an intermetallic system, J. Power Sources 81/82 (1999) 383–387.

[9] S. Bourderau, T. Brousse, D.M. Schleich, Amorphous silicon as a possible anode material for Li-ion batteries, J. Power Sources 81/82 (1999) 233–236.

[10] H. Sakaguchi, H. Honda, T. Esaka, Synthesis and anode behavior of lithium storage intermetallic compounds with various crystallinities, J. Power Sources 81/82 (1999) 229–232.

[11] M. Nishijima, T. Kagohashi, Y. Takeda, M. Imanishi, O. Yamamoto, Eletrochemical studies of a new anode material, $Li_{3-x}M_xN$ (M=Co, Ni, Cu), J. Power Sources 68 (1997) 510–514.

[12] A. Martinez-de la Cruz, N.L. Alcaraz, A.F. Fuentes, L.M. Torres-Martinez, Electrochemical lithium insertion in some niobates MNb_2O_6 (M=Mn, Co, Ni, Cu, Zn and Cd), J. Power Sources 8182 (1999) 255–258.

[13] K. Zaghib, M. Armand, M. Gauthier, Electrochemistry of anodes in solid-state Li-ion polymer batteries, J. Electrochem. Soc. 145 (9) (1998) 3135–3140.

[14] J. Wang, I.D. Raistrick, R.A. Huggins, Behavior of some binary lithium alloys as negative electrodes in organic solvent-based electrolytes, J. Electrochem. Soc. 133 (3) (1986) 457–460.

[15] D. Fauteux, R. Koksbang, Rechargeable lithium battery anodes: alternatives to metallic lithium, J. Appl. Electrochem. 23 (1) (1993) 1–10.

[16] J.O. Besenhard, J. Yang, M. Winter, Will advanced lithium-alloy anodes have a chance in lithium-ion batteries? J. Power Sources 68 (1) (1997) 87–90.

[17] M. Tapiero, S. Tarabichi, J.G. Gies, C. Noguet, J.P. Zielinger, M. Joucla, J.L. Loison, M. Robino, Preparation and characterization of Zn_4Sb_3, Electr. Energy Mater. 12 (1985) 257–274.

[18] S.-G. Kim, I.I. Mazin, D.J. Singh, First-principles study of Zn–Sb thermoelectrics, Phys. Rev. B 57 (11) (1998) 6199–6203.

[19] JCPDS (Joint Committee on Powder Diffraction Standards) No. 34–1013.

[20] X. Zhao, G. Cao, A study on behaviors of lithium-ion inserting in Zn_4Sb_3 anode, Electrochimica. Acta, in preparaton.